XLIII CILAMCE
21–25, November, 2022
FOZ DO IGUAÇU – PR – BRAZIL

Thermoelastic stationary analysis of non-oriented grain steels using BEM

Caio C. C. Moura[1], Andrés F. Galvis[2], Paulo Sollero[1]

[1]*School of Mechanical Engineering, University of Campinas, Campinas, 13083-860, São Paulo, Brazil*
caiomoura@fem.unicamp.br, sollero@fem.unicamp.br
[2]*School of Mathematics and Physics, University of Portsmouth Portsmouth PO5 1NY, United Kingdom*
andres.galvis@port.ac.uk

Abstract. This work deals with a thermoelastic analysis of anisotropic cold-rolled non-oriented grain steels (FeSi) where the material is subjected to severe thermal and inertial loads. Following the stationary thermoelasticity formulation of the boundary element method (BEM), this model focuses on the 2D study of these materials when the elastic properties are temperature-dependent. The cold rolling process promotes a deformed microstructure on steels with 3%Si. After the cold rolling process, this material is subjected to an annealing process to recrystallize the microstructure. This process promotes crystallographic texture in the material, with a strong Goss fiber and weak (hkl)[110] and (111)[uvw] fibers. That is, although classified as non-oriented grain steel after the annealing process, steels with 3%Si produced by the cold-rolled process have crystallographic texture in all stages of manufacturing, resulting in an anisotropic material. An industrial application is shown to illustrate the feasibility of using the presented formulation, and the stationary thermomechanical response of the material. Taking advantage of the BEM capabilities to solve high gradients and secondary mechanical fields within the domain.

Keywords: Thermoelasticity; Boundary element method; Non-oriented grain steel; Anisotropy

1 Introduction

The steady growth in the complexity of engineering projects reflects the present fast technological advancement. To enable projects that are increasingly efficient and competitive, which take into account complex requests, it becomes necessary to use adequate computational tools. It is common for a large amount of equipment, machinery, and even structures to contain components that operate under temperature gradients that give rise to thermoelastic stresses. These stresses are provoked by important engineering phenomena, including fatigue failure and the formation and spread of cracks, as well as other events that jeopardize component structural integrity. Mathematical models that describe the thermoelastic phenomenon can be found in abundance in the literature (Salençon [1]; Gaul et al. [2]; Ieşan [3]). Therefore, it is critical to comprehend these stresses and strains in order to use the proper failure criterion and technical considerations when dimensioning these components.

In order to preserve better fidelity to the original problem, computational modeling techniques must be able to account for all of the major boundary conditions. This faithfulness is closely tied to the safety and dependability of the project. In that cases, it becomes essential to use numerical techniques to approximate solutions for problems with complex requests. The BEM stands out with greater applicability to thermoelastic solutions among the various existing approaches. In this work, a stationary state BEM equation, described by Gaul et al. [2], will be used to solve a thermoelastic problem in a continuum media.

The continuum media analyzed in this work is a non-oriented silicon steel at macroscopic length scale. At the nanoscale, non-oriented silicon steels have body-centered cubic cubic unit cell structure. Each grain is considered as an anisotropic elastic media, with elastic properties varying depending on the lattice structure and chemical composition. At the macroscale, each material point is represented by a set of non-periodic polycrystal aggregates (Nygårds [4]; Kamaya [5]; Galvis et al. [6]). Then, a stochastic morphological grain assembly with its distinct crystalline orientations can be modeled to approximate the macroscopic elastic properties.

In general, studies that evaluated the effects of thermal and inertial loads on non-oriented grain steels approximated the elastic properties as isotropic. However, non-oriented steels produced by the cold-rolled process show orthotropic elastics properties. Deva et al. [7] and Moura et al. [8] observed that the parameters of the cold rolling

process influence the anisotropy of the ferritic steels mechanical properties. In addition, the crystallographic orientation of each grain is not random according to Franke et al. [9]. Cunha and Paolinelli [10] observed peaks of texture intensity at $(110)[001]$, Goss component, and weak γ fiber with peaks close to $(111)[112]$ on a sample of non-oriented silicon steel after recrystallization at the end of the cold-rolled process, indicating that the material has certain predominant crystallographic orientations.

In the present work, a BEM stationary thermoelasticity formulation is applied to evaluate the influences of thermal and inertial effects on a non-oriented silicon steel continuum media, considering the orthotropy of its elastic properties temperature-dependent. The results obtained by numerical integration are compared to results obtained with the exact and finit element method (FEM) solutions.

2 Mathematical model

For a generally anisotropic two-dimension model, the constitutive relationship between the stress σ_{ij} and strain ε_{ij} considering temperature changes is governed by the Duhamel-Neumann relation:

$$\sigma_{ij} = C_{ijkl}\varepsilon_{ij} - \gamma_{ij}\theta, \tag{1}$$

where C_{ijkl} is the material stiffness coefficients, θ is the temperature change, and γ_{ij} is the thermoelastic tensor given by $\gamma_{ij} = C_{ijkl}\alpha_{kl}$, for α_{ij} being the coefficients of linear expansion. According Gaul et al. [2], substituting the equation (1) into Cauchy's equation of motion

$$\sigma_{ij,j} + \varrho b_i = \varrho \dot{v}_i, \tag{2}$$

being ϱ the material density, b_i is a body force of arbitrary nature, and $\dot{v}_i$ the acceleration of the material particle, the field equation of thermoelasticity is obtained in terms of displacements u_i:

$$C_{ijkl}u_{k,lj} - \gamma_{ij}\theta_{,j} + \varrho b_i = \varrho \dot{v}_i. \tag{3}$$

In the case of static thermoelasticity, all physical variables are independent of time; i.e., $\dot{v}_i$ is vanished. Equation (3) then reduces to

$$C_{ijkl}u_{k,lj} - \gamma_{ij}\theta_{,j} + \varrho b_i = 0, \tag{4}$$

where b_i will be considered in this work as a inertial load.

3 Boundary integral equation for stationary thermoelasticity

The boundary integration equation (BIE) in the direct BEM formulation for a two-dimension anisotropic solid, when the temperatures θ or heat flux q are previously known on boundary, provides an integral relation between tractions t_i and displacements u_i on the boundary Γ of the domain Ω. The thermoelastic representation formula is given by (see, e.g. Gaul et al. [2] and Sollero and Aliabadi [11])

$$\begin{aligned} c_{ij}(z_{0k})u_j(z_{0k}) + \int_\Gamma T_{mi}(z_k, z_{0k})u_i(z_k)d\Gamma = \int_\Gamma U_{mi}(z_k, z_{0k})t_i(z_k) \\ + \int_\Gamma U_{mi}(z_k, z_{0k})\gamma_{ij}\theta n_j d\Gamma - \int_\Omega f_i^{el} U_{mi}(z_k, z_{0k})d\Omega, \end{aligned} \tag{5}$$

for

$$f_i^{el} = \gamma_{ij}\theta_{,j} - \varrho b_i. \tag{6}$$

In the equations (5) and (6), the term c_{ij} is given by $\delta_{ij}/2$ for a smooth boundary; T_{mi} and U_{mi} are the fundamental solution for tractions and displacements, respectively, in function of source z_{0k} and field z_k points on Γ of the complex plane. The displacements u_i and tractions t_i are computed on Γ. The displacement fundamental solution is given by

$$U_{mi}(z_k, z_{0k}) = 2Re\left[P_{i1}A_{j1}logz_1 + P_{i2}A_{j2}logz_2\right], \tag{7}$$

and for tractions

$$T_{mi}(z_k, z_{0k}) = 2Re\left[Q_{i1}(\mu_1 n_1 - n_2)A_{j1}/(z_1 - z_{01}) + Q_{i2}(\mu_2 n_1 - n_2)A_{j2}/(z_2 - z_{02})\right], \tag{8}$$

where P_{ij}, Q_{ij}, and A_{ji} are complex constants which depend on the material elastic constants; μ_j is the roots of the characteristic equation of the anisotropic material and Re is the operator to obtain the real part of a complex

result (Sollero and Aliabadi [11] and Lekhnitskii [12]). Lastly, $z(\mu)$ is a generalized complex variable defined in terms of μ and the difference of coordinates between the field x_i and source points x_i^p, given by

$$z = (x_1 - x_1^p) + \mu(x_2 - x_2^p). \tag{9}$$

The volume integral in the right-hand-side of the equation (5) needs to be analytically transformed into boundary integral ones so as to restore the distinctive feature of the BEM as a boundary solution computational technique. The dual reciprocity formulation technique (DRBEM), proposed by Brebbia and Dominguez [13], was used to solve the volume integral. The discretization of the boundary integrals was performed with quadratic continuous boundary elements and the solutions was implemented using FORTRAN language.

4 Results

Non-oriented silicon steels are mainly applied in electrical machines under inertial loads by centrifugal forces and temperature rise without a temperature gradient, i.e., the heat flux is given by $q = -k_{ij}\theta_{,j}n_i$ and equals to zero. For k_{ij} being the thermal conductivity tensor. To satisfy this boundary condition, $\theta_{,j}$ is equals to zero and the therm $\gamma_{ij}\theta_{,j}$ is vanishes from the equation (6). Therefore, de equation (6) becomes

$$f_i^{el} = \varrho b_i. \tag{10}$$

A few numerical examples are presented in this section to test the efficiency of the proposed formulation for stationary thermoelasticity considering inertial and thermal effects on non-oriented silicon steel according to the application in the construction of electrical motor rotors in the form of lamination stacks. The material properties are shown below.

4.1 Material properties

In this work, the elastic properties were experimentally obtained from a sheet sample of a polycrystalline non-oriented silicon steel with 3.3% Si and 0.30 mm of thickness produced by the cold-rolled process. An orthotopic C_{ij} was calculated from experimental results, by the relation $C_{ij} = S_{ij}^{-1}$, for S_{ij} defined by elastic constants and Poisson's ratio of the material, as follows

$$S_{ij} = \begin{bmatrix} 1/E_1 & -v_{21}/E_2 & 0 \\ -v_{12}/E_1 & 1/E_2 & 0 \\ 0 & 0 & 1/G_{12} \end{bmatrix}. \tag{11}$$

The elastic constants and Poisson's ratio were measured experimentally by tensile tests, at room temperature T, performed in a traction test machine INSTRON 5583 according to ASTM E8/E8M standard [14]. To measure the Young's moduli in directions x and y, the Poisson's ratio v_{12} and shear moduli G_{12}, the samples were prepared according to the Figure (1). Sample measurements were made in real time during the tensile test using a displacement point detector.

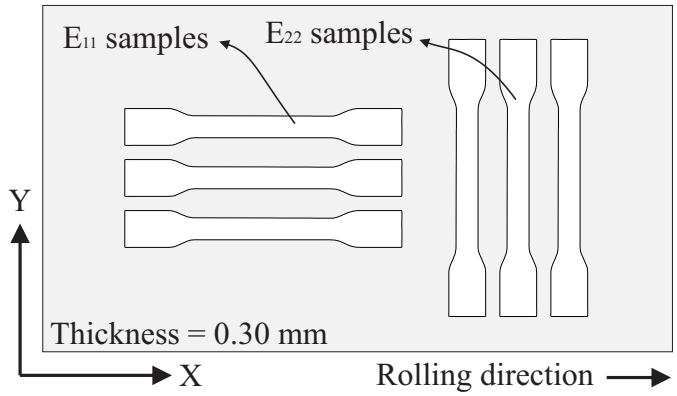

Figure 1. Specimen to obtain the elastic properties in function of principal directions by tensile test.

The temperature-dependence was calculated through the elastic constants into S_{ij} in function of the body temperature during the solution according the equation (12) obtained from the ASME Table A-1 [15] for low and intermediate alloy steels in temperature range $21 \rightarrow 204$ °C. $E(T)$ is Young's modulus in the function of temperature and E_o is Young's modulus in ambient temperature. A low-alloy steel is a type of metal mixture composed of steel and another metals that possess desirable properties. Low-alloy steel contains about $1\% - 5\%$ of alloying elements.

$$E(T) = E_o - 0.018T^{1.235}. \tag{12}$$

The coefficient of thermal expansion α is given by ATI [16] for $20 \rightarrow 300$ °C temperature range. The main properties of the material considered in this work measured in ambient temperature are shown in Table 1.

Table 1. Thermoelastic properties experimentally obtained of a non-oriented silicon steel with 3.3%Si.

E_{11} [GPa]	E_{22} [GPa]	G_{12} [GPa]	v_{12}	α [°C^{-1}](20-300°C)	Density [kg/m³]
162.00 ± 4.50	152.00 ± 2.00	63.28 ± 1.75	0.28	1.29×10^{-5}	7650

4.2 Numerical examples

In the face of the material properties experimentally obtained, the first step in the BEM solution validation procedure consists of numerically comparing exact and FEM solutions to evaluate the accuracy of the results. In this sense, three numerical examples are shown considering thermal, inertial, and tractions as boundary conditions. The elastic properties were considered temperature-dependent in all examples.

Linear thermal expansion in a bar

First, a linear thermal expansion case of a bar is solved in the model showed in Figure 2. The numerical results is compared to the exact solution

$$\Delta L = \alpha L_o \theta, \tag{13}$$

for ΔL being the linear thermoexpansion and L_o the initial length. In this case, the sheet domain was modeled as a square with dimensions equal to 1 m under a thermal load $\theta = 1$ °C/step, displacements in x_1 direction equal to zero on the left and right sides, and fully constraint at the bottom. The BEM discretization was done with 3 discontinuous quadratic boundary elements per edge and 9 equidistant internal points in the domain with (0.5,y) coordinates.

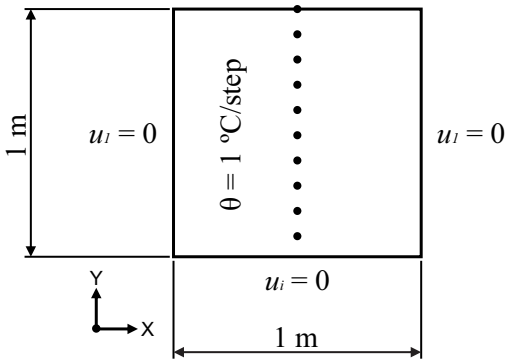

Figure 2. Linear thermoexpansion boundary conditions and the indication of the regions in which the results are shown.

The u_2 results along the internal points until the boundary are shown for the first step analysis in Figure (3). The BEM solution achieved good accuracy in the results when compared to the exact solution. The maximum relative error between BEM results and exact results calculated by equation (13) was 0.36%. Indicating that the BEM results presented an excellent accuracy with the exact solution.

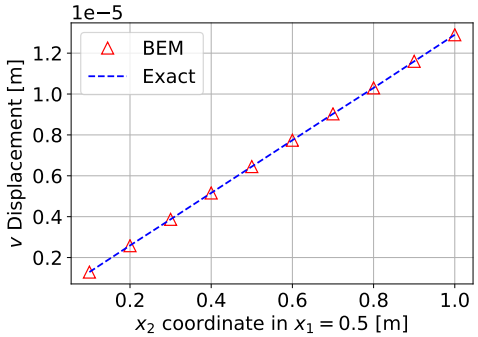

Figure 3. The u_2 results along the internal points until the boundary for the first step analysis for the linear thermoexpansion problem in a bar.

Fixed body under thermal expansion

The domain modeling was kept as a square with dimensions equal to 1 m under a thermal load $\theta = 1$ °C/step. The boundary supports were defined as fully constraint at the bottom and the left-hand side. The BEM discretization was done with 19 discontinuous quadratic boundary elements per edge. The BEM results are compared to a FEM results model with the same boundary conditions solved by the commercial Ansys Mechanical software ®.

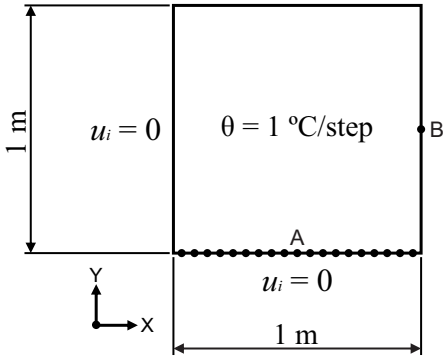

Figure 4. Boundary conditions of the fixed body case and the indication of the regions in which the results are shown.

Figure (5) shows the comparison between BEM and FEM results of the u_1 and u_2 displacements in function of the steps. The BEM solution achieved good accordance in the results when compared to the FEM solution. The maximum error between BEM and FEM results was 0.15% for u_1 (Figure 5a) and 0.85% for u_2 (Figure 5b). In addition, figure (6) showns de comparison between von Mises stress results. The accuracy of the results was satisfactory and the stress gradient obtained in the BEM solution is close to the solution obtained by FEM.

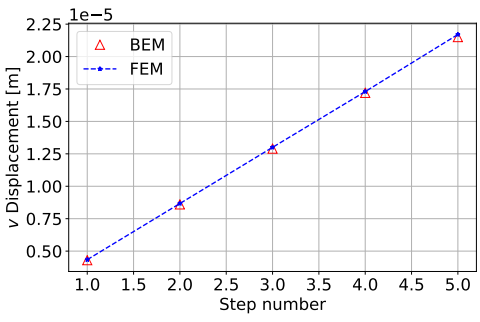

(a) u_1 results at point B.

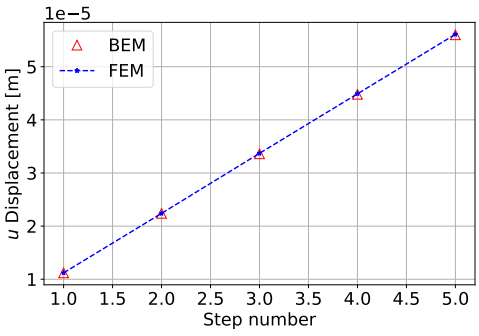

(b) u_2 results at point B.

Figure 5. Comparisons of the BEM and FEM displacement results at points B in function of the step number analysis.

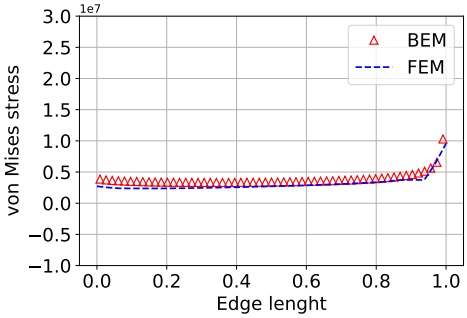

Figure 6. Comparision between FEM and BEM solutions for a recessed boundary on edge A in the first step.

Thermoelastic problem with inertial forces

The domain dimensions are shown at figure (7). The boundary conditions were defined as: fully constraint on the left-hand edge, thermal load $\theta = 1$ °C/step, the body under the action of the acceleration of gravity, and the right-hand edge is under a distributed force where the tractions was defined as $\sigma_{22}n_2 = -200$ Pa. The BEM discretization was done with 11 discontinuous quadratic boundary elements per edge. The BEM results are compared to a FEM results model with the same boundary conditions solved by the commercial Ansys Mechanical software ®.

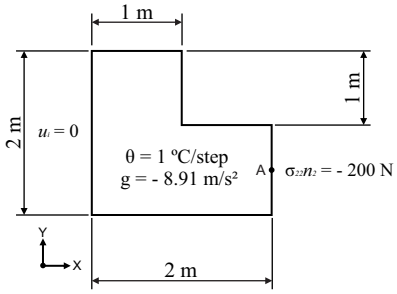

Figure 7. Boundary conditions of the thermoelastic problem with inertial forces case and the indication of the regions in which the results are shown.

Figure (8) shows the comparison between BEM and FEM results of the u_1 and u_2 displacements for all step analysis. As with the examples shown above, BEM displacement results achieved good accordance when compared to the displacement FEM results. The maximum error between BEM and FEM solutions was 0.31% for u_1 results (Figure 8a) and 3.80% for u_2 results (Figure 8b). Focusing on the maximum error obtained in u_2 results, it is possible to notice that, although the error was the largest compared to the results obtained in the other solutions presented in this work, the error variation is still small considering the order of complexity of the boundary conditions for this case.

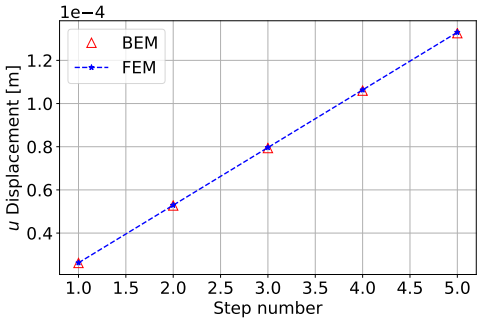

(a) u_1 results at point A.

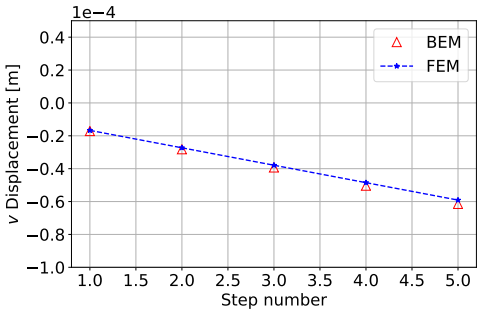

(b) u_2 results at point A.

Figure 8. Comparison of the BEM and FEM displacement results at point A for the thermoelastic problem with inertial forces.

5 Conclusions

This work implemented a BEM stationary thermoelasticity formulation capable of considering thermal and inertial effects on a non-oriented silicon steel continuum media, considering the orthotropy of its elastic properties temperature-dependent. At the end, the small magnitude order of the obtained error value between BEM, exact, and FEM solutions, indicated that the BEM pointed out a good performance.

Acknowledgements. The authors would like to thank to the University of Campinas (Brazil) and University of Portsmouth (UK) for the facilities and structure provided to develop this work. The project was funded by, the Brazilian Coordination for the Improvement of Higher Education Personnel-CAPES (Grant Number: 435214/2019-01). This material is based on work supported by the Air Force Office of Scientific Research-AFOSR under Award Numbers FA9550- 18-1-0113 and FA9550-20-1-0133. Andres F. Galvis was supported by the EPSRC New Investigator Award "Multiscale modelling of mechanical deterioration in lithium-ion batteries" Grant number EP/T000775/1.

Authorship statement. The authors hereby confirm that they are the sole liable persons responsible for the authorship of this work, and that all material that has been herein included as part of the present paper is either the property (and authorship) of the authors, or has the permission of the owners to be included here.

References

[1] J. Salençon. *Handbook of Continuum Mechanics: General Concepts Thermoelasticity*. Springer, 2001.
[2] L. Gaul, M. Kögl, and M. Wagner. *Boundary Element Methods for Engineers and Scientists: An Introductory Course with Advanced Topics*. Springer Berlin Heidelberg, 2012.
[3] D. Ieşan. *Thermoelastic Models of Continua*. Springer, 2004.
[4] M. Nygårds. Number of grains necessary to homogenize elastic materials with cubic symmetry. *Mechanics of Materials*, vol. 35, n. 11, pp. 1049–1057, 2003.
[5] M. Kamaya. A procedure for estimating young's modulus of textured polycrystalline materials. *International Journal of Solids and Structures*, vol. 46, n. 13, pp. 2642–2649, 2009.
[6] A. F. Galvis, R. Q. Rodríguez, and P. Sollero. Analysis of three-dimensional hexagonal and cubic polycrystals using the boundary element method. *Mechanics of Materials*, vol. 117, pp. 58–72, 2018.
[7] A. Deva, P. Pandey, and M. Alam. Processing of low-carbon deep-drawing steel with high plastic anisotropy using two-stage batch annealing cycle. *Journal of Materials Engineering and Performance*, vol. 30, pp. 1612–1618, 2021.
[8] C. Moura, R. Barbosa, and T. Oliveira. Effect of grain size on the drawability of the niobium-stabilized ferritic stainless steel ASTM 430. *Tecnologia em Metalurgia, Materiais e Mineração*, vol. 17, n. 4, pp. 2176–1523, 2019.
[9] A. Franke, J. Schneider, and B. Bacroix. Evolution of microstructure and texture in ferritic Fe-Si steels at final annealing – role of strain induced boundary migration and secondary recrystallization. *Proc. 9. International Conference Magnetism and Metallurgy*, vol. 9, pp. 349, 2020.
[10] M. Cunha and S. Paolinelli. Non-oriented silicon steel recrystalization texture study. *Materials Science Forum*, vol. 408-4123, pp. 779–784, 2002.
[11] P. Sollero and M. Aliabadi. Fracture mechanics analysis of anisotropic plates by the boundary element method. *International Journal of Fracture*, vol. 64, pp. 269–284, 1993.
[12] S. Lekhnitskii. *Theory of Elasticity of an Anisotropic Body*. Central Books, Washington, 1981.
[13] C. Brebbia and J. Dominguez. *Boundary Elements: An Introductory Course*. Boundary Elements: An Introductory Course. Computational Mechanics Publications, 1992.
[14] E8/E8M. Standard test methods for tension testing of metallic materials. Standard, ASTM International, West Conshohocken, 2016.
[15] B31.1-2018. ASME code for pressure piping. Standard, The American Society of Mechanical Engineers, New York, NY, 2018.
[16] Grain-oriented electrical steel technical data sheet. Standard, Allegheny Technologies Incorporated, Pittsburgh, PA, 2018.